JOURNAL OF VIROLOGY, Mar. 2005, p. 3807–3821 Vol. 79, No. 6
0022-538X/05/$08.00+0 doi:10.1128/JVI.79.6.3807–3821.2005

Size Heterogeneity in the 3′ Noncoding Region of South American Isolates of Yellow Fever Virus

Juliet E. Bryant,[1,2] Pedro F. C. Vasconcelos,[3] Rene C. A. Rijnbrand,[1,4] J. P. Mutebi,[5] Stephen Higgs,[1,2] and Alan D. T. Barrett[1,2,4]*

Department of Pathology,[1] Center for Biodefense and Emerging Infectious Diseases,[2] and Department of Microbiology and Immunology,[4] University of Texas Medical Branch, Galveston, Texas; Department of Arbovirology, Instituto Evandro Chagas, Ministry of Health, Belém, Brazil[3]; and Chicago Department of Public Health, Chicago, Illinois[5]

Received 5 August 2004/Accepted 25 October 2004

The 3′ noncoding region (3′ NCR) of flaviviruses contains secondary and tertiary structures essential for virus replication. Previous studies of yellow fever virus (YFV) and dengue virus have found that modifications to the 3′ NCR are sometimes associated with attenuation in vertebrate and/or mosquito hosts. The 3′ NCRs of 117 isolates of South American YFV have been examined, and major deletions and/or duplications of conserved RNA structures have been identified in several wild-type isolates. Nineteen isolates (designated YF-XL isolates) from Brazil, Trinidad, and Venezuela, dating from 1973 to 2001, exhibited a 216-nucleotide (nt) duplication, yielding a tandem repeat of conserved hairpin, stem-loop, dumbbell, and pseudoknot structures. YF-XL isolates were found exclusively within one subclade of South American genotype I YFV. One Brazilian isolate exhibited, in addition to the 216-nt duplication, a deletion of a 40-nt repeated hairpin (RYF) motif (YF-XL-ΔRYF). To investigate the biological significance of these 3′ NCR rearrangements, YF-XL-ΔRYF and YF-XL isolates, as well as other South American YFV isolates, were evaluated for three phenotypes: growth kinetics in cell culture, neuroinvasiveness in suckling mice, and ability to replicate and produce disseminated infections in *Aedes aegypti* mosquitoes. YF-XL-ΔRYF and YF-XL isolates showed growth kinetics and neuroinvasive characteristics comparable to those of typical South American YFV isolates, and mosquito infectivity trials demonstrated that both types of 3′ NCR variants were capable of replication and dissemination in a laboratory-adapted colony of *A. aegypti*.

The 3′ noncoding region (3′ NCR) of flaviviruses contains *cis*-acting sequences that are essential for genome replication and translation. Experimental studies indicate that variations in the 3′ NCR are well tolerated but may sometimes lead to altered growth characteristics in cell culture (3, 6, 19), changes in virulence and immunogenicity in vertebrate animals (10, 17, 21, 22), or reduced infectivity in mosquitoes (1, 44). Molecular epidemiological studies of naturally occurring flaviviruses also suggest that 3′ NCR structural differences correlate with patterns of virus distribution and transmission (39, 50). Size heterogeneity has been observed within the 3′ NCRs of several species of mosquito-borne and tick-borne flaviviruses (12, 32, 39, 48), as well as viruses of the no-known-vector group (5). In addition, it has recently been reported that genome fragments representing a major portion of the 3′ NCR accumulate in Japanese encephalitis virus-infected cell cultures (18). Together, these studies suggest that the 3′ NCR may play a regulatory role in RNA synthesis. Evolutionary divergence of the 3′ NCR is thus of considerable interest, as this region is hypothesized to contain molecular determinants of virulence, cell tropism, and/or host specificity.

Previous studies of the 3′ NCR of yellow fever virus (YFV) have examined variability within a limited number (using up to 14 isolates) of African and South American wild-type isolates (8, 13, 29, 49). These studies have shown that YFV 3′ NCRs vary in length from 444 to 524 nucleotides (nt) and contain a series of repeated hairpin motifs (designated RYFs; ~40 nt) that are genotype specific in number. Sequences examined to date reveal three RYFs among West African isolates of YFV, two RYFs among East African isolates of YFV, and only one RYF among South American isolates of YFV (28, 49). Similar well-conserved and type-specific hairpin repeats are also found among closely related flaviviruses of the YFV genetic group (28). The function of the RYFs remains obscure; indeed, little is known of the biological importance of individual structural components within the 3′ NCR.

The flavivirus 3′ NCR comprises several hairpin-loop structures whose secondary structures are well conserved across virus species, although the primary nucleotide sequences are highly divergent (34). The 3′ NCR has been divided into three regions based on differing levels of sequence conservation (Fig. 1): domain I is the region immediately following the stop codon that is hypervariable and contains insertions-deletions (indels) in most flavivirus species; domain II is a region of moderate conservation comprising several hairpin motifs, including a characteristic dumbell structure and CS2 motif (~24 nt) present in all mosquito-borne flaviviruses; and domain III is the highly conserved essential region, containing a cyclization domain (~8 to 14 nt) and the terminal long stable hairpin (~90 nt), which are essential for viral replication (34, 35). Size heterogeneity among flaviviruses is mostly due to sequence repeats or deletions within domain I. RNA structures within domains I and II are considered dispensable for virus replication (3, 19, 22). However, because deletion mutants typically exhibit some degree of growth restriction or attenuation (3,

* Corresponding author. Mailing address: Department of Pathology, University of Texas Medical Branch, Galveston, TX 77555-0609. Phone: (409) 772-6662. Fax: (409) 772-2500. E-mail: abarrett@utmb.edu.

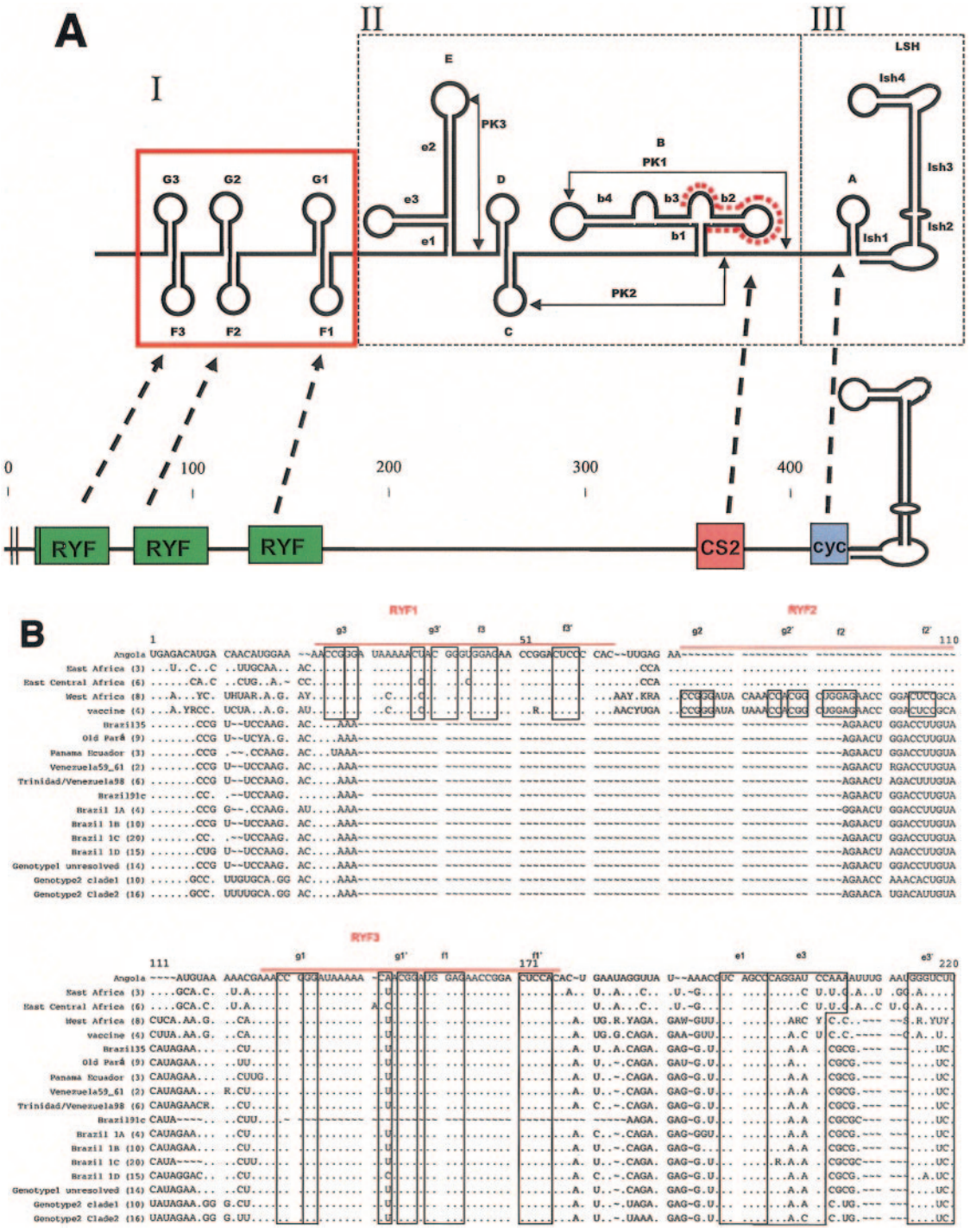

FIG. 1. (A) Schematic diagram highlighting conserved features of the prototype YFV 3′ NCR (modified from reference 28). RYF, repeated dual F-G hairpins; CS2, ~24 nt comprising part of dumbbell B; cyc, conserved cyclization domain; LSH, long stable hairpin. (B) Consensus alignment of YFV 3′ NCR sequences (domains I and II). The numbers of isolates used to build the consensus sequences are provided in parentheses (details in Table 1). Nucleotides identical to the reference Angola71 isolate are indicated by dots. Alignment was optimized by the insertion of gaps (~). Ambiguity codes are as follows: M = A or C; R = A or G; W = A or T; S = C or G; Y = C or T; K = G or T; V = A, C,or G; H = A, C, or T; D = A, G, or T; B = C, G, or T. Regions involved in basepairing are boxed and labeled to correspond with stem structures as indicated in the schematic in panel A.

22), the structures of domains I and II are believed to serve as replication enhancer elements. The evolutionary conservation of RNA secondary structures across numerous species of mosquito-borne flaviviruses also strongly suggests that they play an important role in virus replication. Based on comparative sequence analysis of 14 wild-type YFV isolates and 7 vaccine isolates, Proutski et al. (33, 34) suggested an association between the predicted folding structure of the 3′ NCR (in par-

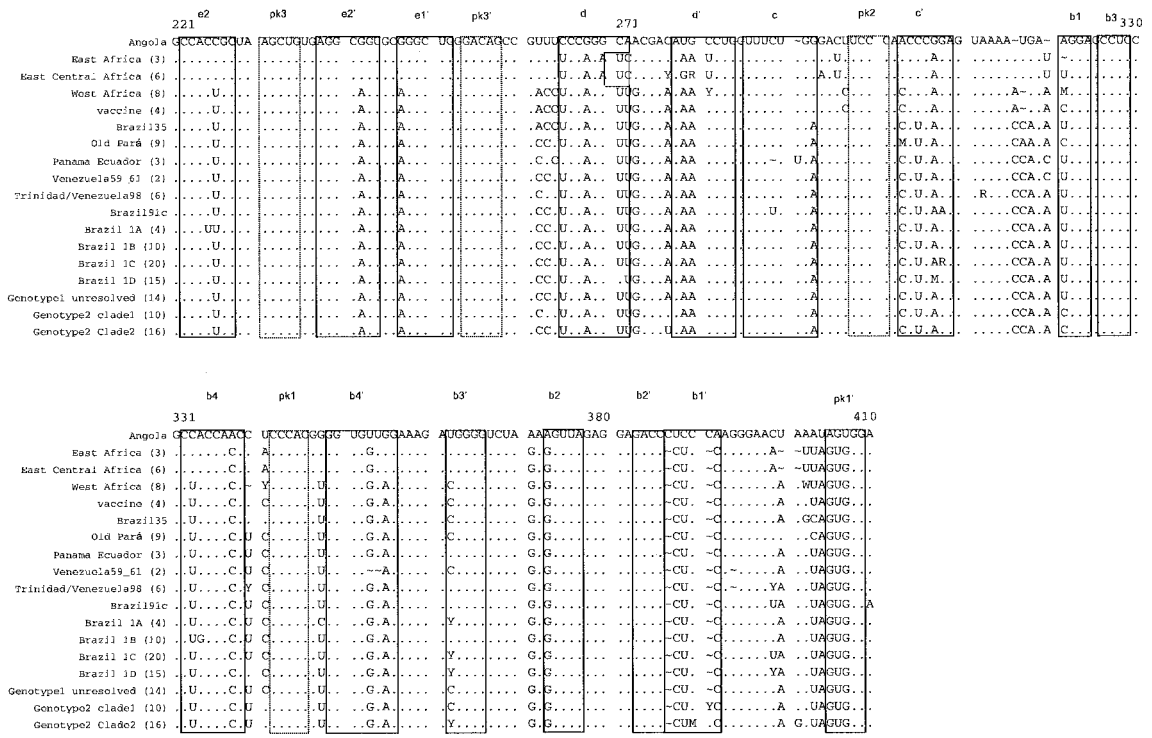

FIG. 1—*Continued.*

ticular, the long stable hairpin of domain III and the e3 stem-loop of domain II) and the virulence of YFV.

In the present study, novel 3′ NCR sequence data for 112 South American and 8 African YFV isolates were generated. Sixteen previously published YFV 3′ NCR sequences were incorporated into the data set for a combined total of 136 sequences. The data were interpreted within the context of predicted RNA folding patterns as determined by Proutski et al. (34) and Olsthoorn and Bol (30). Our examination focused primarily on South American YFV isolates, because preliminary work revealed a novel 3′ NCR conformation (YF-XL) among a subset of South American genotype I viruses. The YF-XL conformation consisted of an imperfect tandem repeat of RNA structures within domain II of the 3′ NCR. In addition, the 3′ NCR of one South American genotype I isolate containing the YF-XL repeat was found to lack all three RYFs (YF-XL-ΔRYF). To investigate the functional significance of the YF-XL 3′ NCR conformation, the growth characteristics of the variant isolates were evaluated in cell culture, suckling mice, and *Aedes aegypti* mosquitoes. The natural history of duplications and deletions in the 3′ NCR of YFV was examined through phylogenetic reconstructions and interpreted within the context of present models for RNA recombination. The results of this study may have important implications for the molecular evolution of YFV, as they underscore the significant genomic plasticity of the 3′ NCR and suggest a possible role of RNA structural features in promoting template switching during virus replication.

MATERIALS AND METHODS

Virus isolates used in this study. The wild-type isolates of YFV used in this study were made available through the University of Texas Medical Branch World Arbovirus Reference Center. The majority of South American isolates were low-passage sylvan isolates of virus originally isolated at the Instituto Evandro Chagas in Belém, Brazil, and at the Instituto Nacional de Salud in Lima, Peru. The sources, geographic origins, and passage histories of isolates for which 3′ NCR sequences were obtained, as well as information on isolates with previously published data, are provided in Table 1. The majority of isolates were made via passage in suckling mouse brain, followed by amplification in C6/36 cell culture, and had minimal passages following primary isolation.

RT-PCR and sequencing. The methods for genomic RNA extraction and amplification of viral sequences by reverse transcriptase (RT) PCR were as previously described (49) with the following modifications. RNA extraction was achieved using the QIAamp Viral RNA Mini kit (QIAGEN) according to the manufacturer's instructions, and the reverse transcription protocol employed Superscript II RNase H^- RT (Invitrogen). Sequences of the genome terminus were obtained using either the sNS5i-aNS5i or the emf-vd8 primer pairs. The sNS5i primer amplifies from genomic positions 10167 to 10188 (5′-CCAAGAG ACAAGACAAGCTGTG-3′); aNS5i binds to the genome terminus positions 10838 to 10862 (5′-AGTGGTTTTGTGTTTTTCATCCAAAG-3′); emf corresponds to positions 10055 to 10075 (5′-TGGATGACSACHGARGAYA-3′), and vd8 binds to 10709 to 10728 (5′-TAGAGGTTAGAGGAGACCC-3′). Amplicons were visualized by gel electrophoresis, gel extracted (QIAGEN gel extraction kit), and sequenced by direct sequencing using a Perkin-Elmer 373XL. Sequences were obtained from both strands of each RT-PCR amplicon for sequence confirmation (using the same primers for amplification reactions). Amplicons of isolates that did not produce sufficient quantities for direct sequencing were cloned into the pGEM-EZ cloning vector (Promega); three clones were sequenced in both directions to provide a representative consensus sequence.

Sequence analysis. Initial editing of 3′ NCR sequence fragments was performed using Vector NTI (Informax). Sequences were aligned and manually edited using the Genomics Computer Group Wisconsin Package version 10.3 (Accelrys, Inc., San Diego, Calif.). The PAUP* program (41) was used to infer maximum-likelihood trees of the multiple sequence alignment.

Growth characteristics in cell culture. Twelve-day growth curves for YF-XL and YF-XL-ΔRYF, as well as representative South American genotype I and II isolates with "standard" 3′ NCR conformations (YF-std), were determined in C6/36 and Vero cells. Cell monolayers at 75 to 80% confluency were incubated with virus stock at an approximate multiplicity of infection (MOI) of 0.03 for 1 h at 37 (Vero) or 28°C (C6/36). After the 1-h incubation, the monolayers were

TABLE 1. Viruses used in this study

Isolate	Strain	Passage level[a]	Source	State[b]	Genotype, clade[c]	3′ NCR status[d]	GenBank no.	Reference
14 FA	Angola71	SM7 Mosq 1	Human	ND	Angola	YF-std	AY326413	28
OBS 7687	Bolivia99A	C6/36#2	Human	Santa Cruz	SAm II, clade 2	YF-std	AY541326	
OBS 8026	Bolivia99D	C8/36#2	Human	La Paz	SAm II, clade 1	YF-std	AY541327	
JSS	Brazil35	Mosq1, SM8	Human	MT	SAm I, Old Pará	YF-std	U52389	49
BeH 111	Brazil54	C6/36, SM10	Human	PA	SAm I, Old Pará	ND	AY541335	4
BeAr 162	Brazil56B	SM4, C6/36#1	*Haemagogus janthinomys*	PA	SAm I, Old Pará	YF-std	AY541336	46a
BeAr 189	Brazil55C	SM1 C6/36#1	*Sabethes* sp.	PA	SAm I, Old Pará	YF-std	AY541337	4
BeAn 23536	Brazil60	SM1 C6/36#1	*Macaco* sp.	PA	SAm I, Old Pará	ND	AY541338	4
BeAr 46299	Brazil62A	C6/36#1	*Haemagogus* sp.	PA	SAm I, Old Pará	YF-std	AY541339	4
BeAr 44824	Brazil62B	SM1 C6/36#1	*Haemagogus* sp.	PA	SAm I, Old Pará	ND	AY541340	4
BeAn 142028	Brazil68A	C6/36#1	*Macaco* sp.	PA	SAm I, Old Pará	YF-std	AY541341	4
BeAr 142658	Brazil68C	SM2, C6/36#1	*Haemagogus* sp.	PA	SAm I, Old Pará	YF-std	AY541342	4
BeAn 142027	Brazil68D	Original	*Saguinus midas*	PA	SAm I, Old Pará	YF-std	AY566272	4
BeH 171995	Brazil69A	SM1 C6/36#1	Human	PA	SAm I, unresolved	ND	AY541343	46a
BeH 203410	Brazil71	Original, C6/36#1	Human	PA	SAm I, clade 1C	ND	AY541344	4
BeAr 233164	Brazil73A	Mosq 4	*H. janthinomys*	GO	SAm I, clade 1A	YF-XL	AY541345	4
BeAn 232669	Brazil73B	Mosq 1, SM2	*Mosquito*	GO	SAm I, clade 1A	YF-std	AY541346	4
BeAr 233436	Brazil73C	Original	*Haemagogus* sp.	GO	SAm I, clade 1A	ND	AY541347	4
BeH 233393	Brazil73D	SM1 C6/36#1	Human	GO	SAm I, clade 1A	ND	AY541348	46a
BeAr 301129	Brazil76A	SM1 C6/36#1	*Haemagogus* sp.	PA	SAm I, unresolved	ND	AY541349	46a
BeH 301035	Brazil76B	SM1 C6/36#1	Human	PA	SAm I, unresolved	ND	AY541350	46a
BeH 324213	Brazil77	SM1 C6/36#1	Human	PA	SAm I, unresolved	ND	AY541351	46a
BeH 350698	Brazil78A	SM2, Mosq 1	Human	PA	SAm I, clade 1C	ND	AY541352	4
BeAr 350397	Brazil78B	SM2, Mosq 1	*Haemagogus* sp.	PA	SAm I, unresolved	YF-XL	AY541353	46a
BeH 340824	Brazil78C	SM1 C6/36#1	Human	PA	SAm I, unresolved	ND	AY541354	46a
BeH 371220	Brazil79A	SM1 C6/36#1	Human	PA	SAm I, unresolved	ND	AY541355	46a
BeAr 378600	Brazil80A	SM2, C6/36#1	*Haemagogus* sp.	GO	SAm I, clade 1C	ND	AY541356	46a
BeH 385780	Brazil80B	SM1 C6/36#1	Human	PA	SAm I, unresolved	YF-XL	AY541357	46a
BeH 379501	Brazil80C	SM2	Human	MA	SAm I, clade 1C	ND	AY541358	4
BeH 394880	Brazil81	Original, C6/36#1	Human	PA	SAm I, unresolved	ND	AY541359	46a
BeH 403366	Brazil82A	SM1 C6/36#1	Human	MA	SAm I, clade 1C	ND	AY541360	46a
BeH 405954	Brazil82B	SM1 C6/36#1	Human	PA	SAm I, unresolved	ND	AY541361	46a
BeH 413820	Brazil83	SM1 C6/36#1	Human	RO	SAm II, clade 1	YF-std	AY566273	46a
BeH 425381	Brazil84A	C6/36#1	Human	AP	SAm I, unresolved	ND	AY541362	4
BeAn 424208	Brazil84B	Original, C6/36#1	*Chiropotes satanas*	PA	SAm I, clade 1C	ND	AY541363	46a
BeAr 424719	Brazil84C	SM1 C6/36#1	*Haemagogus* sp.	PA	SAm I, clade 1C	ND	AY541364	46a
BeAr 424083	Brazil84D	SM1 C6/36#1	*Haemagogus albomaculatus*	PA	SAm I, clade 1D	ND	AY541365	46a
BeAr 424492	Brazil84E	SM1 C6/36#1	*H. janthinomys*	PA	SAm I, clade 1A	ND	AY541366	46a
BeH 422255	Brazil84F	SM1 C6/36#1	Human	PA	SAm 1, clade 1B	ND	AY541367	46a
BeH 423602	Brazil84G	SM1 C6/36#1	Human	PA	SAm I, clade 1C	ND	AY541368	46a
BeH 422312	Brazil84H	SM1 C6/36#1	Human	PA	SAm 1, clade 1B	ND	AY541369	46a
BeH 436823	Brazil85A	SM1 C6/36#1	Human	MT	SAm I, unresolved	ND	AY541370	46a
BeAr 437159	Brazil85B	SM1 C6/36#1	*H. janthinomys*	MT	SAm I, unresolved	ND	AY541371	46a
BeH 463676	Brazil87	SM1 C6/36#1	Human	PA	SAm I, clade 1C	ND	AY541372	46a
BeH 474245	Brazil88A	SM1 C6/36#1	Human	GO	SAm I, clade 1C	ND	AY541373	46a
BeH 474297	Brazil88B	SM1 C6/36#1	Human	MG	SAm I, clade 1C	ND	AY541374	46a
BeH 485717	Brazil89	SM1 C6/36#1	Human	MG	SAm I, clade 1C	ND	AY541375	46a
BeAr 511437	Brazil91A	C6/36#1	*H. janthinomys*	PA	SAm I, clade 1C	ND	AY541376	4
BeH 511843	Brazil91B	SM1, C6/36#2	Human	RR	SAm I, clade 1B	YF-XL	AY541377	4
BeAn 510266	Brazil91C	SM1 C6/36#1	*Alouatta* sp.	GO	SAm I, clade 1C	YF-ΔRYF-XL	AY541378	46a
BeAr 512943	Brazil92A	SM1 C6/36-1 Vero2	*H. janthinomys*	MS	SAm 1, clade 1B	YF-XL	AY541379	4
BeAr 513008	Brazil92B	SM1 C6/36#1	*Sabethes* sp.	MS	SAm 1, clade 1B	YF-XL	AY541380	4
BeH 512772	Brazil92C	SM2, C6/36#1	Human	MS	SAm 1, clade 1B	ND	AY541381	4
BeAr 513060	Brazil92D	SM1 C6/36#1	*Haemagogus* sp.	MS	SAm 1, clade 1B	YF-XL	AY541382	46a
BeAr 513292	Brazil92E	SM1 C6/36-1 Vero1	*Sabethes cloropterus*	MS	SAm 1, clade 1B	YF-XL	AY541383	4
BeH 520988	Brazil93A	SM1 C6/36#1	Human	MA	SAm 1, clade 1B	YF-std	AY541384	46a
BeH 521244	Brazil93B	SM1 C6/36#1	Human	MA	SAm I, clade 1C	YF-XL	AY541385	46a
BeAr 527785	Brazil94A	SM1 C6/36#1	*S. cloropterus*	MG	SAm I, clade 1C	YF-XL	AY541386	4
BeAr 527198	Brazil94B	SM1 C6/36#1	*Haemagogus* sp.	MG	SAm I, clade 1C	YF-XL	AY541387	4
BeAr 527547	Brazil94C	?, Vero1	*Haemagogus* sp.	PA	SAm I, clade 1C	ND	AY541388	46a
BeH 526722	Brazil94D	SM2, C6/36#1	Human	MG	SAm I, clade 1C	YF-std	AY541389	46a
BeAr 528057	Brazil94E	Original, C6/36#1	*H. janthinomys*	MG	SAm I, unresolved	ND	AY541390	46a
BeAr 527410	Brazil94F	Original, C6/36#1	*H. janthinomys*	MA	SAm I, clade 1C	ND	AY541391	46a
BeH 535010	Brazil95	SM2, C6/36#1	Human	MA	SAm I, clade 1C	ND	AY541392	46a
BeAr 544276	Brazil96A	SM1 C6/36#1	*H. janthinomys*	RO	SAm 1, clade 1B	YF-XL	AY541393	4
BeAn 604552	Brazil98A	Original, C6/36#1	*Alouatta belzebul*	PA	SAm 1, clade 1C	ND	AY541394	46a
BeAr 603401	Brazil98B	Original, C6/36#1	*H. janthinomys*	PA	SAm 1, clade 1D	ND	AY541395	46a
BeAr 605158	Brazil98C	SM1 C6/36#1	*H. janthinomys*	PA	SAm 1, clade 1D	ND	AY541396	46a
BeH 603325	Brazil98D	Original, C6/36#1	Human	PA	SAm 1, clade 1D	ND	AY541397	46a
BeH 605427	Brazil98E	SM1 C6/36#1	Human	MT	SAm 1, clade 1D	ND	AY541398	46a
BeAr 614320	Brazil99B	SM1 C6/36#1	*Haemagogus* sp.	PA	SAm 1, clade 1D	ND	AY541399	46a

Continued on facing page

TABLE 1—*Continued*

Isolate	Strain	Passage level[a]	Source	State[b]	Genotype, clade[c]	3′ NCR status[d]	GenBank no.	Reference
BeAr 617127	Brazil99D	SM1 C6/36#1	*H. janthinomys*	TO	SAm 1, clade 1D	ND	AY541400	46a
BeH 613582	Brazil99E	SM1 C6/36#1	Human	PA	SAm 1, clade 1D	ND	AY541401	46a
BeAr 628124	Brazil2000A	SM1 C6/36#1	*H. janthinomys*	TO	SAm 1, clade 1D	YF-std	AY541328	4
BeH 622491	Brazil2000B	?, C6/36#1	Human	DF	SAm 1, clade 1D	ND	AY541329	46a
BeAn 625923	Brazil2000C	Original, C6/36#1	*Alouatta* sp.	GO	SAm 1, clade 1D	ND	AY541330	46a
BeH 622205	Brazil2000D	SM1 C6/36#1	Human	GO	SAm 1, clade 1D	ND	AY541331	46a
BeAr 630768	Brazil2001A	?, C6/36#1	*H. janthinomys*	GO	SAm 1, clade 1D	ND	AY541332	46a
BeAr 631464	Brazil2001B	SM1 C6/36#1	*S. cloropterus*	BA	SAm 1, clade 1D	YF-XL	AY541333	46a
BeAr 645693	Brazil2001D	SM1 C6/36#1	*Haemagogus* sp.	MG	SAm 1, clade 1D	ND	AY541334	46a
Ar B 8883	CAR77A	SM5, C6/36#1	Mosquito	Boyo	East Central Africa	ND	U52392	4a
Ar B 9005	CAR77B	SM5 Mosq1	*Aedes africanus*	Boyo	East Central Africa	ND	U52395	4a
DAK Ar B 17239	CAR80	AP61#1, C6/36#1	*Aedes* sp.	Bozo	East Central Africa	ND	AY541402	
V528A	Colombia79	Monkey 1 Mosq2	Human	ND	SAm I, unresolved	ND	AY541403	
INS347613	Colombia85	C6/36#3	Human	ND	SAm I, unresolved	ND	AY541404	
1337	Ecuador79	SM1, Mosq2	Human	ND	SAm I, unresolved	YF-std	U52399	4a
1345	Ecuador81	SM1, Vero1, c6/36#2	Human	ND	SAm I	ND	AY541405	
OBD 5041	Ecuador97	C6/36#1	Human	Pastaza	SAm II, clade 1	YF-std	AY541406	
Serie 227	Ethiopia61A	Mosq1, SM7	Human	ND	East Africa	ND	AY541407	
Asibi	Ghana27	C6/36#1	Human	ND	West Africa II	ND	Not deposited	37a
85-82H	IvoryCoast85	?, C6/36#1	Human	ND	West Africa II	ND	O54798	49
BC 7914	Kenya93a	SM1, c636#1	Human	Baringo	East Africa	ND	AY541408	
69056	Nigeria46	?, C6/36#2	Human	ND	West Africa I	ND	U52403	29
IB AR 45244	Nigeria69	SM4	Mosquito	ND	West Africa I	ND	AY541409	
H117505	Nigeria87C	SM4	Human	ND	West Africa I	ND	AY541410	
56205	Nigeria91	?, C6/36#1	Human	ND	West Africa I	ND	AY541411	
614819	Panama74A	?, C6/36#1	Human	ND	SAm I	YF-XL	AY541412	
1362/77	Peru77A	C6/36#2	Human	Ayacucho	SAm II, clade 2	YF-std	AY541413	4
1368	Peru77B	SM1, Vero1, C6/36#2	Human	Ayacucho	SAm II, clade 1	ND	AY541414	4
1371	Peru77C	SM1, Vero1, C6/36#2	Human	Ayacucho	SAm II, clade 2	ND	AY541415	4
287/78	Peru78	SM2, Mosq 2	Human	Ayacucho	SAm II, clade 2	ND	AY541416	4
R 35740	Peru79	SM1, Mosq 2	Human	Ayacucho	SAm II, clade 2	ND	AY541417	4
B4.1	Peru81A	Plaque pick	Plaque pick	Cusco	SAm II, clade 2	YF-std	U52411	4a
1914	Peru81B	MILLC 1, LLCMK2	Sentinel mice	Cusco	SAm II, clade 2	ND	AY541418	4
ARV 0544	Peru95A	SM1, Vero1, c6/36#1	Human	S. Martin	SAm II, clade 1	YF-std	AY541419	4
HEB4224	Peru95B	SM1, C6/36#1	Human	S. Martin	SAm II, clade 1	ND	AY541420	4
HEB4236 (153)	Peru95C	C6/36#1	Human	Pasco	SAm II, clade 2	YF-std	AY541421	4a
149	Peru95D	SM1, C6/36#1	Human	Pasco	SAm II, clade 2	YF-std	AY541422	4a
cepa #2	Peru95E	SM1, C6/36#1	Human	Puno	SAm II, clade 2	YF-std	AY541423	4
Cepa#1	Peru 95F	C6/36#2	Human	Puno	SAm II, clade 1	ND	AY541424	4
OBS 2240	Peru95G	C6/36#2	Human	Huanuco	SAm II, clade 1	YF-std	AY541425	4
OBS 2250	Peru95H	SM1, C6/36#1	Human	Huanuco	SAm II, clade 2	ND	AY541426	4
HEB 4240	Peru95I	C6/36#1, SM1	Human	Junin	SAm II, clade 2	ND	AY541427	4
HEB 4245	Peru95J	SM1, C6/36#1	Human	Junin	SAm II, clade 2	ND	AY541428	4
HEB 4246	Peru95K	SM1, C6/36#1	Human	Junin	SAm II, clade 2	YF-std	AY541429	4
ARV 0548	Peru95M	SM1, C6/36#1	Human	S. Martin	SAm II, clade 1	ND	AY541430	4
OBS 6530	Peru98A	?, C6/36#1	Human	Cusco	SAm II, clade 2	ND	AY541431	4
03-5350-98	Peru98B	C6/36#2	Human	Cusco	SAm II, clade 2	ND	AY541432	4
OBS 6745	Peru98C	C6/36#2	Human	Cusco	SAm II, clade 2	YF-std	AY541433	4
IQT 5591	Peru98D	C6/36#2	Human	Loreto	SAm II, clade 1	ND	AY541434	4
OBS 7904	Peru99	Vero1, C6/36 3	Human	S. Martin	SAm II, clade 1	YF-std	AY541435	4
FVV	Senegal27	Monkey, c6/36#1	Human	ND	West African II	ND	GI694115	49a
Dak 1279	Senegal65C	SM7	Human	ND	West African II	ND	U52413	49
M 90-5	Sudan40B	C6/36#1, SM4	Human	ND	East Central Africa	ND	AY326414	28
GML902621	Trinidad54	Monk1, C6/36#1	*Alouatta* sp.	ND	SAm I, unresolved	ND	AY541436	
CAREC 889920	Trinidad88	AP61#2, C6/36#1	*Haemagogus* sp.	S.E. Trin	SAm I	YF-XL	AY541437	
CAREC 890692	Trinidad89A	?, C6/36#1	*S. cloropterus*	S.E. Trin	SAm I	YF-XL	AY541438	
CAREC 891957	Trinidad89C	AP61, C6/36#1	*Alouatta* sp.	S.E. Trin	SAm I	ND	AY541439	
A 709-4-A2	Uganda48A1	C6/36#1	Human	ND	East Africa	ND	U52424	
MR 896	Uganda48B1	C6/36#1	Human	ND	East Africa	ND	U52422	
Z 19039	Uganda72	C6/36#1, SM3	Monkey	ND	East Central Africa	ND	AY541440	
P128MC	Venezuela59	SM3, Mosq 1	Monkey	Cojedes	SAm 1	ND	AY541441	
PHO 42H	Venezuela61	C6/36#2, SM2	Human	Tachira	SAm 1	YF-std	AY541442	
35720	Venezuela98A	Vero#1, C6/36#1	Human	Amazonas	SAm I	YF-XL	AY541443	
35708	Venezuela98B	SM1, Vero1	Human	Amazonas	SAm I	YF-XL	AY541444	
STA-LSF-4-4143	Zaire58	SM2, Mosq 1, C6/36#1	Human	ND	East Central Africa	ND	AY541445	

[a] Passage of seed stock virus, cell line, or animal model followed by passage number. SM, suckling mouse; Monk, monkey; Mosq. mosquito. Question mark indicates unknown passage level prior to collection catalogue.

[b] AP, Amapa; BA, Bahia; DF, Federal District; GO, Goiás; MA, Maranhão; MG, Minas Gerais; MS, Mato Grosso do Sul; MT, Mato Grosso; PA, Para; RO, Rondônia; RR, Roraima; TO, Tocantins; ND, no data.

[c] SAm I, South American genotype I; SAm II, South American genotype II.

[d] YF-XL, viruses containing the 216-nt duplication; YF-std, viruses with prototype conformation of 3′ NCR; ND, no data, viruses for which the genome terminus has not been sequenced.

washed twice with phosphate-buffered saline and then incubated in 2% minimal essential medium. Aliquots of the supernatant were harvested with replacement for the subsequent 12 days, and titrations were performed by endpoint infectivity assay in Vero cells.

Mouse neuroinvasiveness studies. The ability of YFV isolates to be neuroinvasive in 8-day-old mice was evaluated following intraperitoneal inoculation. Serial 10-fold dilutions of virus in phosphate-buffered saline were inoculated intraperitoneally into litters of outbred NIH Swiss mice and observed over a period of 15 days. Fifty percent lethal dose (LD_{50}) calculations were performed as described by Reed and Muench (37).

Mosquito infectivity trials. The abilities of YF-XL and YF-XL-ΔRYF isolates to replicate and produce disseminated infections in *A. aegypti* mosquitoes were tested using a white-eyed strain that is known to be highly susceptible to YFV infection (24). Four groups of 50 female *A. aegypti* mosquitoes were orally infected with a YF-XL isolate (Brazil92e), YF-XL-ΔRYF (Brazil91c), Asibi (Ghana27), or vaccine isolate 17D. The Asibi and 17D isolates served as positive and negative controls, respectively; the 17D vaccine virus is incapable of disseminating from the midgut to peripheral body tissues (23). Mosquitoes were exposed to YFV by feeding on infected blood meals consisting of equal volumes of virus and medium containing defibrinated sheep blood and 2 mM ATP as a phagostimulant. Virus inocula were in the form of supernatants from infected Vero cell cultures harvested at 4 (for Asibi, 17D, and Brazil91c) and 9 (for Brazil92e) days postinfection. Ten-day-old female mosquitoes were starved for 24 h prior to the infectious meal and then allowed to feed for 45 min through a chicken skin membane covering a Hemotek feeding apparatus (Discovery Workshops, Accrington, Lancashire, United Kingdom) containing the feeding mixture maintained at 37°C. The fully engorged mosquitoes were sorted and maintained for 14 days at 28°C and 80% humidity. The titer of the infectious meal was determined by direct sampling of the fresh blood meal, as well as by sampling one engorged mosquito (day zero) from each treatment group; titrations were performed by endpoint infectivity assay in Vero cells. All mosquitoes were processed as follows. Heads and bodies were separated and triturated in 140 μl and 1 ml of 2% minimal essential medium, respectively. The body and head homogenates were filtered using a 0.22-μm-pore-size filter (Millipore, Molsheim, France), and virus infection of mosquitoes was determined by RT-PCR. Midgut infection rates (MIR) and disseminated infection rates (DIR) were calculated as the ratio of percent infected over total mosquitoes tested.

RESULTS

Genetic variability of the YFV 3′ NCR. Alignment of all available 3′ NCR sequences for wild-type YFV isolates included 136 sequences (117 South American and 19 African) (Table 1) and required extensive manual editing for indels ranging from 4 to 216 nt in length. As it was not feasible to show an alignment of all 136 sequences, we have combined groups of related viruses in Fig. 1B for clarity and simplicity. The overall conformation of 3′ NCR RNA secondary structures as previously defined (30, 33) appeared to be well conserved among both South American and African isolates of YFV (Fig. 1B). Substitutions that distinguished South American isolates from African isolates are indicated in Fig. 2A. Variable sites were found more frequently in single-stranded regions than in regions with predicted secondary structures (36) (Fig. 2B). The greatest divergence between South American and African isolates occurred within the 5′ side loop (e3) of structure E (Fig. 2A). The e3 region is composed of 22 sites (among African YFVs) and 21 sites (among South American YFVs). Of these sites, 13 were conserved and 9 were variable, making this the region with the highest density of substitutions within the stem-loop structures of the 3′ NCR.

As predicted, domain I of the 3′ NCR was hypervariable, with numerous single-nucleotide polymorphisms in the single-stranded region upstream of the F-G dual-hairpin RYF motifs and size variation resulting from deletions of 40 to 80 nt between the different genotypes (49). The 117 South American isolates contained a single RYF motif, whereas East African isolates contained two RYFs and West African isolates contained three RYFs (28, 49). However, one South American genotype I isolate (Brazil91c; YF-XL-ΔRYF) had a deletion of 45 nt from positions 61 to 106 of the 3′ NCR, thus removing the RYF (F-G dual hairpin) plus an additional 10 nt of downstream single-stranded RNA (Fig. 1B). This isolate was obtained from a fatally infected *Alouatta* monkey in 1991 in Goias State, Brazil. Another notable polymorphism was a 4-nt deletion (3′ NCR positions 178 to 181) in the single-stranded region immediately upstream of the RYF dual hairpin, found in each of the 20 isolates of the Brazil clade 1C (represented as a single sequence in Fig. 1B), as well as in Brazil91C. Two isolates, Trinidad79b and Brazil60, exhibited substitutions in the pk2′ binding site of the C loop that are potentially disruptive to the formation of this pseudoknot structure (data not shown). In these isolates, the corresponding pk2 that binds to pk2′ lacked a covariant change. Similarly, 15 South American isolates exhibited a G→U substitution in stem D, but only one isolate (Brazil91b) showed a compensatory change to preserve the D stem without introducing a bulge (data not shown). The cumulative effect of these substitutions on the RNA folding patterns and secondary structure of the 3′ NCR is unclear.

Structural elements of domain II are duplicated in selected genotype I isolates. Nineteen of the 89 South American genotype I isolates of YFV (21%) were found to contain a duplication of 216 nt from positions 182 to 400 of the 3′ NCR (designated YF-XL). The presence of the YF-XL conformation was initially detected as a double banding pattern observed upon RT-PCR using the emf-vd8 primer pair (Fig. 3A). Sequence analysis of subcloned emf-vd8 band size variants revealed the presence of a duplication; subsequently, confirmation of the duplication was achieved by sequencing sNS5i-aNS5i amplicons (Fig. 3B). The sNS5i forward primer binds to genomic positions in the NS5 coding region, and the aNS5i reverse primer binds to the extreme 3′ genomic terminus; thus, sNS5i-aNS5i amplicons span the entire 3′ NCR and allow analysis of the junction sites at either end. The YF-XL duplication comprised an imperfect repeat of the RNA structures within domain II of the 3′ NCR, including four hairpins (E, D, C, and B) and binding sites for two pseudoknots (pk2 and pk1). The repeat region commenced 3 nt upstream of the E1 stem and ended immediately after the pk2 motif located downstream of dumbbell B. Insertion breakpoints were 100% conserved among the 19 YF-XL isolates at both the 3′ and 5′ ends of the duplication. Alignment of the upstream and downstream copies of the duplicated region revealed variation at a total of 63 sites (29%) over the length of the duplicated region (216 nt; genomic positions 10533 to 10749; 3′ NCR 182 to 400 [Asibi reference numbering]) (Fig. 4). Thirteen variable sites were due to indels. The duplicates within each YF-XL isolate varied at 8.2 ± 4.7 sites. Notable substitutions included a G→U transversion at 3′ NCR position 197 in downstream copies of 16 of the YF-XL isolates; for this position, there was no covariant substitution to help preserve the predicted stem of structure D. In addition, pseudoknot binding sites (pk2 and pk2′) of the upstream sequence differed from the downstream copy in six YF-XL isolates (Brazil92a, -b, -d, and -e; Brazil93b; and Brazil96a) (Fig. 4; also see Fig. 6). The typical pk2-pk2′ interaction of YF-std isolates involved predicted complementary

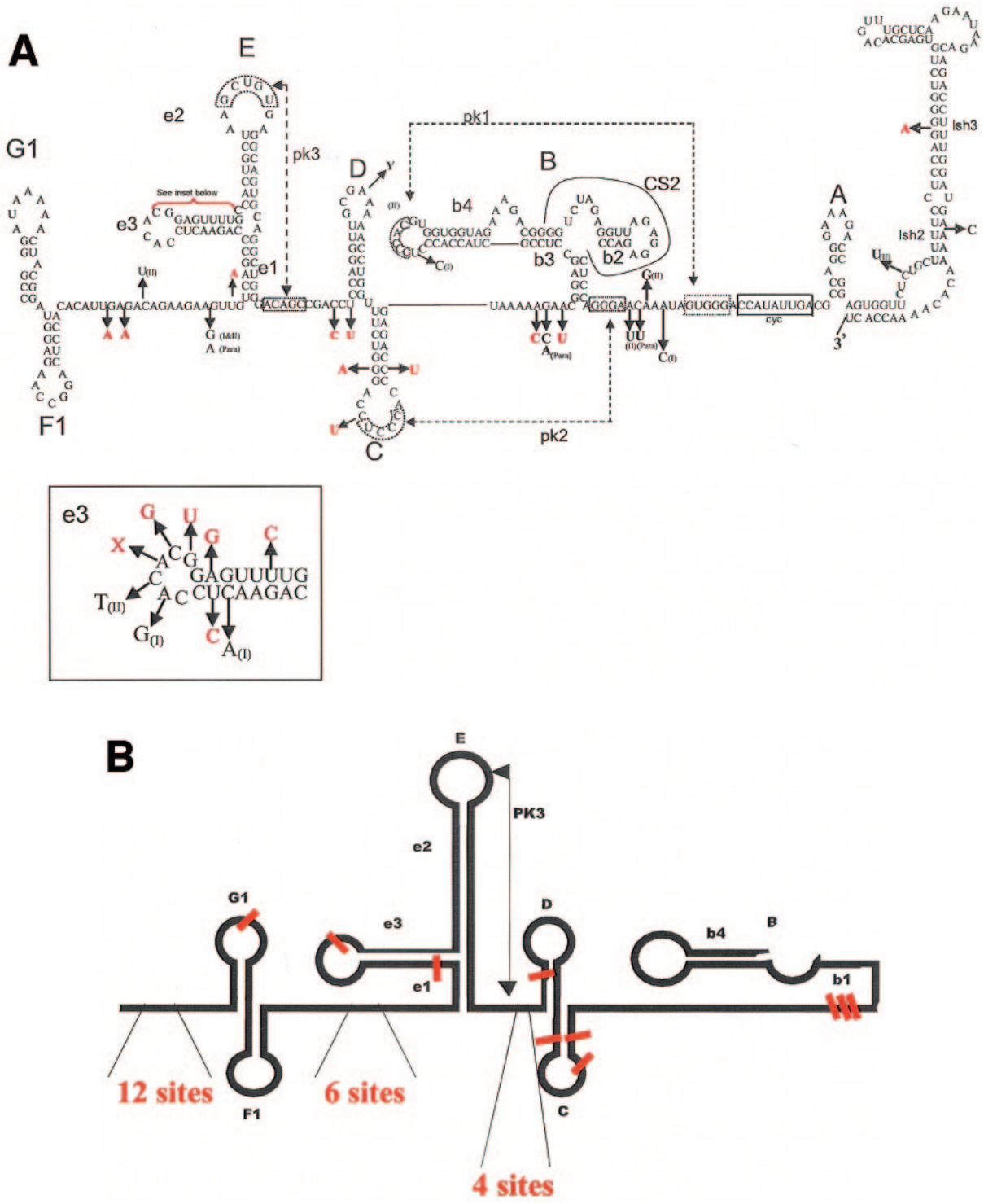

FIG. 2. (A) Nucleotide substitutions within the 3′ NCR of South American YFVs compared to the prototype Asibi isolate. Substitutions shared among all South American isolates are indicated in red; sites that are partially conserved within genotypes I and II are indicated in black. (B) Schematic diagram showing the positions of informative sites within multiple sequence alignment of partial 3′ NCR sequences. Note that the alignment ends after the b4 loop.

binding between a UCCC motif in the loop of structure C and GGGA sequence on the 3′ side of dumbbell B. In these six YF-XL isolates (Brazil92a, -b, -d, and -e; Brazil93b; and Brazil96a), which were closely related variants of the IB clade (see Fig. 6), covariant substitutions in the pk2-pk2′ sites of the duplicated region were evident: C→U at position 226 of the 3′ NCR in the loop of structure C and a G→A substitution at position 323 in pk2′ (Fig. 4). As a result, an altered pseudoknot interaction was possible, involving 5 rather than 4 bp (UUUCC to GGAAA) (Fig. 2A).

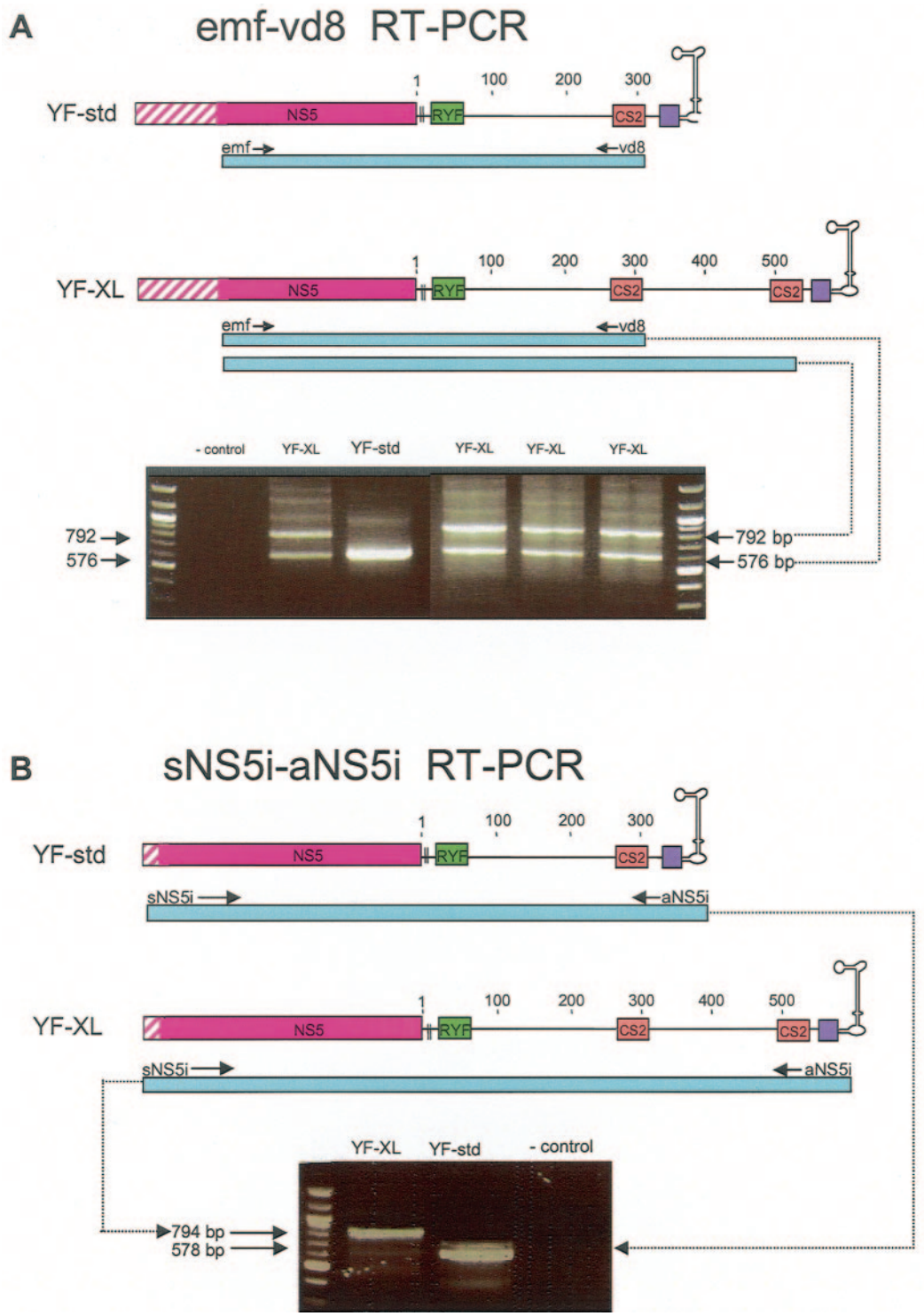

FIG. 3. RT-PCR amplification of YF-XL isolates using the emf-vd8 primer pair results in double bands (A), whereas amplification using the sNS5i-aNS5i primer pair results in a larger fragment size (B).

Growth characteristics in cell culture. To determine the growth characteristics for representatives of the different YF 3′ NCR variants, we infected mosquito C6/36 cells and mammalian Vero cells. The cells were infected at an MOI of 0.03, and infectivity titers in the media were followed for 12 days. Four YF-std and four YF-XL strains were evaluated in duplicate. YF-std isolates grew faster and reached higher peak titers than YF-XL isolates in mosquito cells but not in mammalian cells (Fig. 5). On 10 of the 12 sampling days, titers for the YF-std isolates grown in the C6/36 cultures exceeded those of YF-XL

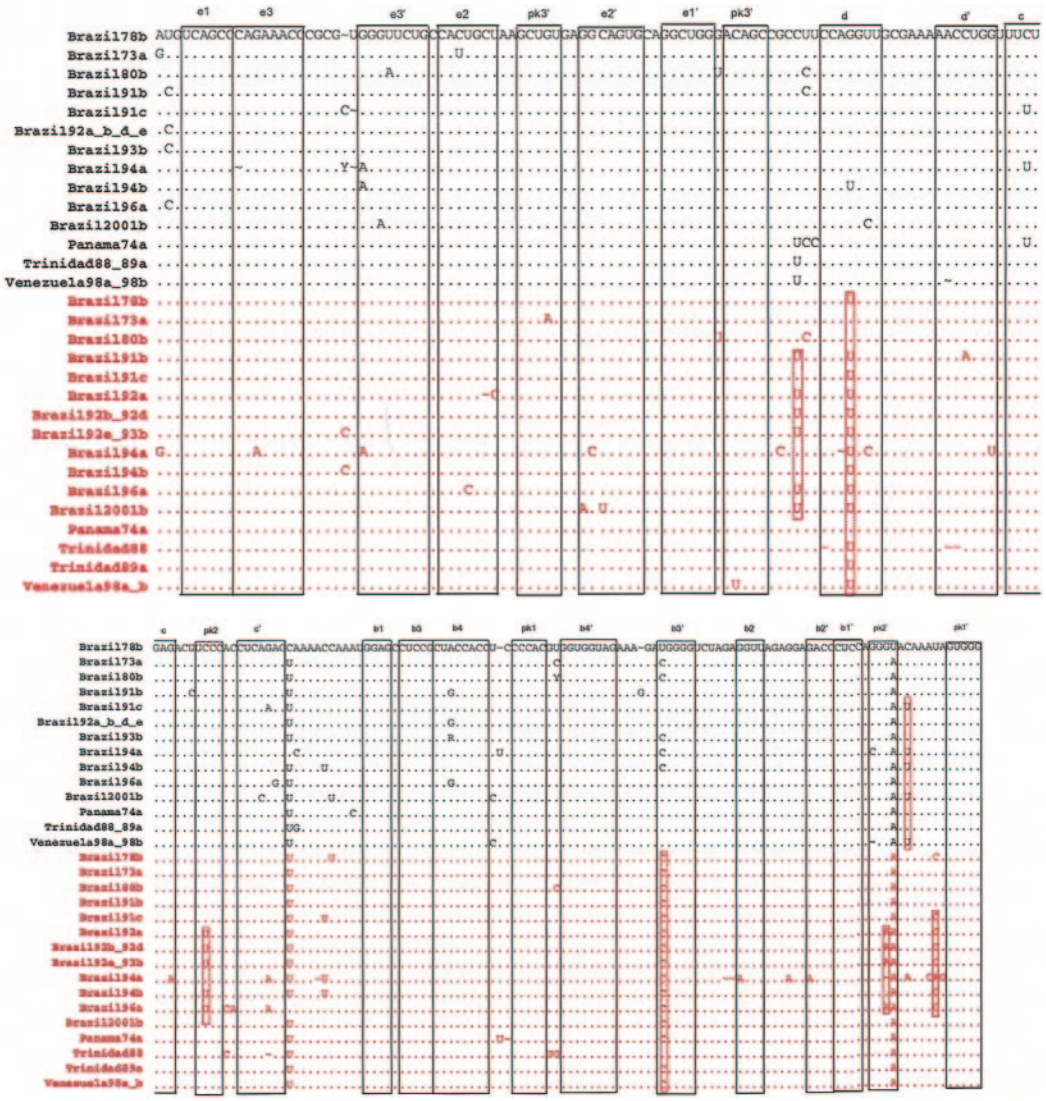

FIG. 4. Alignment of the duplicated region of 19 YF-XL isolates, genomic positions 10533 to 10749 (3′ NCR 182 to 398; Asibi reference numbering). Sequences shown in red are the downstream duplicates of the sequences shown in black. Multiple isolates with 100% identity are represented by a single sequence. Regions involved in basepairing are boxed and labeled to correspond to stem structures as indicated in Fig. 1A and 2A. Hatched boxes indicate pseudoknot binding sites; red boxes indicate conserved substitutions among duplicated structures.

isolates by an average of 1.2 ± 0.5 $\log_{10}$ 50% tissue culture infective dose ($TCID_{50}$) units/ml; however, differences in daily titers were statistically significant only on day 3 ($P = 0.04$), reflecting an ~24-h delay in growth kinetics. There was no evident trend in different growth rates of YF-std and YF-XL in Vero cells (Fig. 5E). The YF-XL-ΔRYF isolate (Brazil91c) grew better than other YF-XL isolates in C6/36 cells, but not in Vero cells. Average peak titers for YF-XL-ΔRYF (5.6 and 5.2 $\log_{10}$ $TCID_{50}$ units/ml in C6/36 and Vero cells, respectively) were equivalent to those observed for YF-std isolates.

Mouse neuroinvasiveness. The abilities of YFV strains to be neuroinvasive in suckling outbred mice were evaluated following intraperitoneal inoculation of 8-day-old litters, as that is the age previously determined to allow optimal discrimination of neuroinvasiveness among strains (11). LD_{50} values were obtained for a total of 10 YF-XL strains (including YF-XL-ΔRYF), 5 YF-std South American genotype I strains, and 7 YF-std South American genotype II strains. LD_{50} values and average survival times for the 22 isolates of South American wild-type YFV revealed significant heterogeneity in the mouse neuroinvasiveness phenotype (Table 2). In general, the neuroinvasiveness phenotype did not appear to be correlated with the genotype or 3′ NCR conformation; there was no significant difference between the lethality of YF-XL (LD_{50} = 3.3 ± 1.3 $\log_{10}$ $TCID_{50}$) and YF-std (LD_{50} = 2.5 ± 1.9 $\log_{10}$ $TCID_{50}$) isolates or between South American genotype I (LD_{50} = 2.6 ± 2.6 $\log_{10}$ $TCID_{50}$) and genotype II (LD_{50} = 2.5 ± 1.3 $\log_{10}$ $TCID_{50}$). Brazil91c (YF-XL-ΔRYF) yielded an LD_{50} of 3.8 $\log_{10}$ $TCID_{50}$. The average survival times were remarkably consistent across all isolates tested (average, 10.2 ± 1.1 days).

Growth characteristics in mosquitoes. Experiments were performed to determine the abilities of YF-XL and YF-XL-ΔRYF strains to produce disseminated infections in Rexville D *A. aegypti*. (Rexville D is a laboratory strain of *A. aegypti* orig-

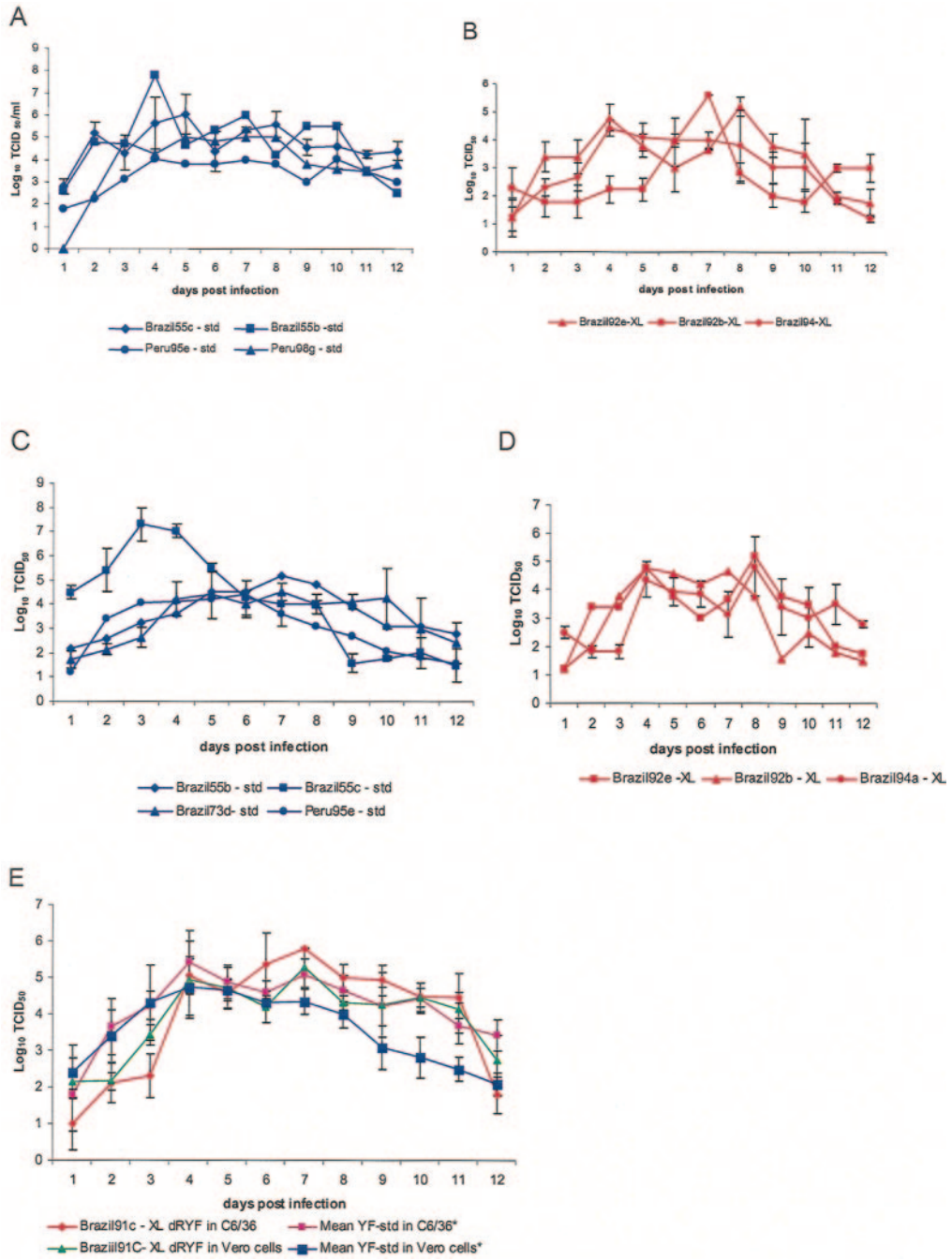

FIG. 5. Comparison of growth characteristics of YF-XL, YF-XL-ΔRYF, and YF-std isolates in Vero and C6/36 cells. Cultures were infected with equal volumes of virus stocks at an approximate MOI of 0.03; 0.5-ml aliquots of supernatant were sampled with replacement for 12 consecutive days. The values represent the mean infectivity titers by endpoint assay; error bars indicate the standard deviations of the results for triplicate samples. (A) YF-std in C6/36 cells; (B) YF-XL in C6/36 cells; (C) YF-std in Vero cells; (D) YF-XL in Vero cells; (E) YF-XL-ΔRYF compared to mean of four YF-std isolates, each evaluated in duplicate.

inally established using mosquitoes from Rexville, Puerto Rico.) Four treatment groups of mosquitoes were orally infected with a representative YF-XL strain (Brazil92e); YF-XL-ΔRYF (Brazil91c); Asibi (prototype West African strain; positive control); and vaccine strain 17D-204 (negative control). Midgut infection rates for YF-XL-ΔRYF and YF-XL were 81 and 89% (Table 3), respectively, and were similar to the infection rate observed for the positive control (Asibi; 80% MIR). There was no evidence of infection in mosquitoes that fed on 17D-204 vaccine (0% MIR; 0% DIR). Dissemination to head tissues was highest in mosquitoes infected with Asibi (61% DIR) and lower in mosquitoes infected with the YF-XL-ΔRYF and YF-XL isolates (35 and 28% DIR, respectively).

Evolutionary relationships among YF-XL isolates. Partial 3′ NCR fragments (~570 nt) were obtained for 73 South American isolates, and complete 3′ NCR sequences (440 to 660 nt)

TABLE 2. Mouse neuroinvasive phenotypes of selected wild-type strains of YFV following intraperitoneal inoculation into litters of 8-day-old mice

Sequence	Strain	Source	Passage history[a]	Log_{10} $TCID_{50}$	LD_{50} (log_{10} $TCID_{50}$)	Avg survival time (days)
South American genotype I						
Brazil55B	BeAR 162	*Haemagogus janthinomys*	SM4, C6/36#1	4.8	0.1	9.2
Brazil60	BeAN 23536	Monkey	SM1, C6/36#1	6.8	5.5	1
Brazil68C	BeAR 142658	*Haemagogus* sp.	?, C6/36#1	6.8	5.5	8.8
Brazil73B	BeAN 232869	Mosquito	Mosq 1, SM2	2.2	0.9	10.2
Venezuela61	PHO 424	Human	C6/36#2, SM2	6.4	0.9	9
South American genotype I-XL						
Brazil73A	BeAN 233164	*Haemagogus*	Mosq 4	4.2	3.7	10.4
Panama74B	Jimenez	Human	Mk1	5.3	0.9	10.2
Brazil73D	BeH 233393	Human	SM1 c6/36#1	4.8	2.6	12
Brazil91C	BeAN 510268	*Alouatta*	SM1 c6/36#1	4.5	3.8	11
Brazil92A	BeAR 512943	*Haemagogus*	C6/36#1	5.0	3.9	10.4
Brazil92B	BeAR 513008	*Sabethes*	SM1, C6/36#1	4.5	4.3	6
Brazil92D	BeAR 513060	*Haemagogus*	SM1, C6/36#1	4.0	1.7	10.2
Brazil92E	BeAR 513292	*Sabethes*	SM1, C6/36#1	6.8	5.3	9.1
Brazil94A	BeAN 527785	*Sabethes*	SM1, C6/36#1	5.0	4.1	9.5
Trinidad89A	CAREC 890692	*Sabethes*	(NH) C6/36#1	4.4	2.8	10.7
South American genotype II						
Bolivia99A	OBS 7687 (JR 035)	Human	C6/36#2	5.6	1.9	9.3
Peru77A	1362/77	Human	C6/36#2	4.6	2.7	9.3
Peru78	287/78	Human	SM1: Mosq 2	4.8	1.8	8.5
Peru81A	B4.1	Human	plaque pick	5.8	2.8	9.1
Peru95a	ARV 0544	Human	SM1, Vero1, C6/36#1	3.8	1.2	10.8
Peru95C	153 (HEB4236)	Human	C6/36#1	7.3	1.9	8.4
Peru95J	HEB 4245	Human	SM1, C6/36#1	5.8	5.3	10.8

[a] Passage history of seed strain in collection. SM, suckling mouse; Mosq, mosquito; Mk, monkey; ham, hamster.

were obtained for 46 South American isolates. Among those isolates for which complete 3′ NCR sequences were obtained, 19 viruses (41%) were identified as YF-XL. The YF-XL isolates originated from the eastern and western states of Brazil (Goiás, Pará, Roraima, Mato Grosso do Sul, Maranhao, Minas Gerais, Rondônia, and Bahia), as well as Trinidad, Venezuela, and Panama (Table 1). YF-XL isolates were found exclusively among the dominant lineage of presently circulating South American genotype I viruses and were not present among the older Brazilian isolates from Pará state dating from 1954 to 1968 (9 isolates) or among South American genotype II isolates (29 isolates) (Fig. 6). The oldest isolate with the YF-XL conformation dated from 1973. There was no apparent correlation between the presence of the YF-XL repeat and the source of the isolate (i.e., mosquito or primate species) or any correlation with passage history. Four of the seven human isolates identified as YF-XL were obtained from fatal human cases (Table 1).

Although YF-XL isolates were confined to one subclade of genotype I, they did not appear to be monophyletic (Fig. 6), and closely related isolates did not appear to share the same 3′ NCR status. There was one instance in which a pair of isolates (Brazil73a and -b) were 100% identical over the partial NS5-3′ NCR fragment (576 nt); however, Brazil73a exhibited the YF-XL conformation and Brazil73b was YF-std (Fig. 6). The prM/E sequences of Brazil73a and Brazil73b were shown to differ by as much as 3.5% (24 nt) (4). Similarly, a group of mosquito isolates from Mato Grosso do Sul were each confirmed as YF-XL (Brazil92a, -b, -d, and -e), but the sequence of the closely related Brazil93a isolate did not show evidence of the duplication.

DISCUSSION

Data presented here provide the first evidence of variation (216 nt) in the length of domain II of the YFV 3′ NCR (YF-

TABLE 3. Oral infection rates of *A. aegypti* (Rexville D) with four strains of YFV[a]

Sequence	Strain	Blood meal titer[b]	Engorged day 0 midgut titer[b]	MIR (% infected midguts) (*n*)[c]	DIR (% infected heads) (*n*)[c]
Ghana27	Asibi	4.2	4.1	80 (5)	61.1 (18)
17D	Vaccine strain	5.6	5.2	0 (14)	0 (13)
Brazil91c (YF-XL-ΔRYF)	BeAN 510268	3.3	3.8	80.7 (26)	35.3 (17)
Brazil92e (YF-XL)	BeAR 513292	2.8	3.9	89.2 (28)	28.5 (21)

[a] The titer for 17D on day zero indicates that mosquitoes ingested live virus at the time of taking the blood meal, but it does not imply or suggest that infections were established within the midgut at this time. In order to demonstrate infection of the midgut, mosquitoes must test positive for viruses after a 2-week incubation period.
[b] log_{10} $TCID_{50}$/ml determined by endpoint assay in Vero cells.
[c] By RT-PCR. *n*, number of females.

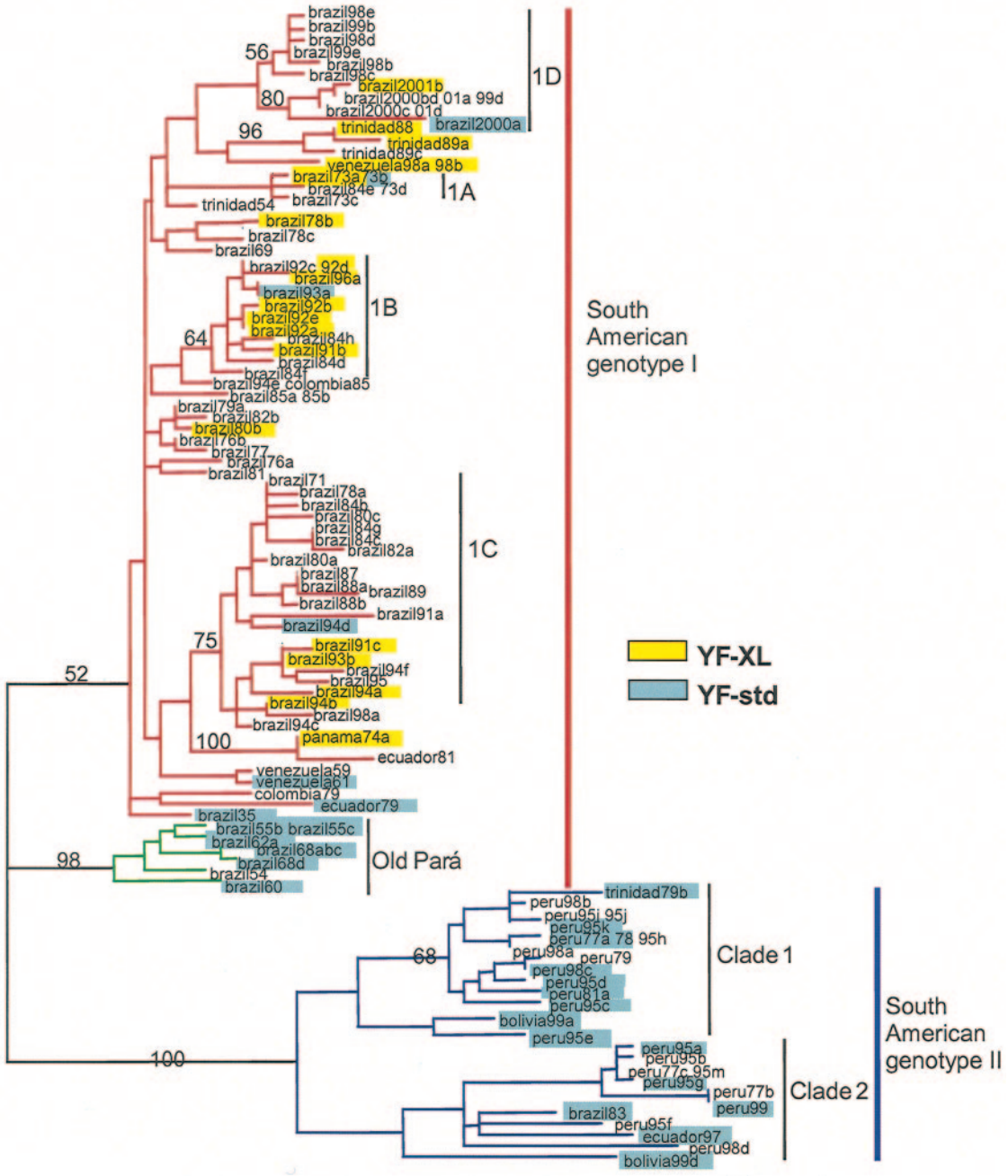

FIG. 6. Neighbor-joining phylogenetic tree based on partial NS5-3′ NCR sequences (576 nt) of 117 South American isolates. To obtain sequences of identical lengths, the alignment was trimmed at the 3′ side of pk1′; thus, the alignment did not incorporate the duplicate copy of domain II structures for the YF-XL isolates. Sequences with 100% identity are represented by single branches. Isolates with no color highlighting have undetermined 3′ NCR status, because sequence for the genome terminus was not obtained.

XL) and the first report of a naturally occurring wild-type YFV strain lacking all three copies of RYF (YF-XL-ΔRYF). The breakpoints of the duplicated regions of the YF-XL strains coincided precisely with predicted structural features. Specifically, the 5′ junction occurred at the base of stem-loop E, and the 3′ junction was immediately upstream of the cyclization motif at the beginning of zone III. There are several critical questions to be addressed regarding the finding of novel 3′ NCR duplications. Most important is whether YF-XL isolates represent naturally occurring virus populations or whether these findings reflect artifactual changes during cell growth or viral amplification by RT-PCR.

Three observations from the sequence data argue against the possibility that YF-XL sequences were generated during RT-PCR amplification. First, the YF-XL sequences were obtained using two different primer pairs (emf-vd8 and sNS5i-aNS5i) (Fig. 3). The sNS5i-aNS5i primer pair generated intact full-length 3′ NCR fragments containing the duplicated regions, whereas the emf-vd8 primer pair generated two fragments, corresponding to fragments both with and without the

repeat. Second, an in vitro enzymatic process cannot easily explain the accumulation of conserved point mutations in the duplicated region. Third, the presence of precise breakpoints among YF-XL isolates suggests an in vivo replication process in which selection has operated to preserve the integrity of specific secondary structures. The presence of precise breakpoints provides indirect evidence in support of the presently proposed model for YFV RNA folding patterns (30, 33).

More difficult to discern is whether the YF-XL duplication may have occurred as a cell culture adaptation during laboratory passage. The YF-XL isolates identified in this study originated from at least four different regional reference laboratories (Instituto Evandro Chagas in Brazil, Gorgas Memorial Laboratory in Panama, Trinidad Regional Virus Laboratory, and the Instituto Nacional de Salud in Venezuela). Isolation procedures for the majority of YFV isolates were uniform (1 passage in suckling mouse brain, followed by growth in C6/36 cells), and most were low passage (<5 passages). Viruses with the XL duplication were found exclusively among isolates from one subclade of South American genotype I, suggesting that the duplication was a unique characteristic of one lineage rather than the result of shared passage histories. It is worth noting that spontaneous deletion of two RYF elements has been reported during passage of a YF vaccine virus (French neurotropic vaccine) (28), and deletions in the 3′ NCR have also been reported following repeated passage of tick-borne flaviviruses (12). Although passage-induced sequence deletions may be a relatively frequent occurrence, the generation of novel duplications is likely to be a rarer event (31). To date, passage-induced duplications have not been reported for any viruses in the genus *Flavivirus*. Definitive proof of the existence of YF-XL in nature will require direct amplification from field-collected material (sera or tissue of infected humans, wild-caught vertebrates, or mosquitoes).

The two copies of domain II RNA structures in YF-XL strains contained an average of 7.6 (3.5%) nucleotide differences. Importantly, a number of substitutions within the duplicated region appeared to be partially conserved (Fig. 4). A pair of covariant substitutions observed in six YF-XL isolates was predicted to increase the complementary interactions of pseudoknot binding (pk2-pk2′) and may serve to differentiate the two pseudoknot binding sites of the duplicated region (Fig. 4). The upstream copy showed higher identity to the homologous region of prototype South American isolates, suggesting that this copy may represent the progenitor sequence. It is particularly interesting that the YF-XL conformation contained two dumbbell structures, since all mosquito-borne flaviviruses studied to date—with the exception of YFV—also contain two dumbbells in domain II of the 3′ NCR (20, 30). Thus, identification of YF-XL isolates suggests the possibility of convergent evolution toward a conformation commonly held by most other mosquito-borne flaviviruses. In viruses of the Japanese encephalitis and dengue serogroups, the two dumbbells are adjacent to one another but separated by flanking A-rich single-stranded regions. In contrast, the spacing between the two dumbbells of YF-XL isolates is significantly greater, due to the intervening duplicated C, D, and E hairpins.

Interestingly, there are two published reports in the clinical and diagnostic literature of aberrant large-size amplicons obtained during analysis of the 3′ NCR of South American YFV (7, 9). These reports involved fatal cases of YF in an unvaccinated tourist who became infected while visiting Manaus, Brazil, in 1997 (9) and within a YF outbreak in Minas Gerais, Brazil, in 2001 (7). Both reports used RT-PCR emf-vd8 amplification to identify South American genotype I isolates, and both reported unexpected double bands from sample viruses but not from controls (wild-type and attenuated West African isolates). The large bands were dismissed as PCR artifacts; however, no apparent attempts were made to sequence the fragments. These findings indirectly support the hypothesis that the extra bands (YF-XL) are characteristic of South American genotype I YFV. To date, complete 3′ NCR sequences have been obtained for a total of 46 South American YFV isolates, and 19 (41%) have shown evidence of the YF-XL duplication, as confirmed by multiple sequencing reactions. As mentioned previously, the YF-XL isolates have been identified exclusively from the dominant lineage of contemporary South American genotype I isolates (Fig. 6). Sequence determinations for the remaining South American genotype I isolates will likely reveal more examples of the YF-XL 3′ NCR conformation.

Growth characteristics of YF-XL isolates. Because RNA secondary structures of the 3′ NCR are involved in virus replication and are believed to serve as replication enhancer elements (22, 30, 33, 47), it was hypothesized that YF-XL isolates would exhibit a phenotype measurably different from those of YF-std isolates in one or more model systems (i.e., cell culture, suckling mice, or mosquitoes). Evaluation of South American YFV isolates in the mouse model showed no significant difference among the neuroinvasive properties of YF-XL, YF-XL-ΔRYF, and YF-std isolates (Table 2) or differences in lethality between South American genotype I YFV ($n = 15$) and South American genotype II ($n = 7$). The YF-XL-ΔRYF isolate showed cell culture growth characteristics similar to those of YF-std isolates in both C6/36 cells and monkey kidney Vero cells. In contrast, three representative YF-XL isolates grew more slowly than YF-std isolates in *Aedes albopictus* mosquito larval C6/36 cells, but not in monkey kidney Vero cells. The observation that YF-XL isolates exhibited delayed replication in C6/36 cells suggests the possibility that the duplicated domain II RNA secondary structures either directly or indirectly influence replication efficiency within cell lines of arthropod origin. Nevertheless, the YF-XL isolate Brazil92e and YF-XL-ΔRYF Brazil91c successfully established midgut and disseminated infections in *A. aegypti* mosquitoes following oral feeding on infectious blood meals (Table 3). MIRs for YF-XL and YF-XL-ΔRYF were 89 and 81%, respectively, and DIRs were 28 and 35%, respectively (Table 3). The infectivity of these strains was particularly remarkable given the relatively low titer of the infectious blood meal, which was 1 log unit lower than for 17D-204. Previously published studies using Rexville D *A. aegypti* mosquitoes have estimated MIRs for South American YFV in the range of 42 to 100% and DIRs from 46 to 79% (14, 24–26). Thus, the infectivity rates of YF-XL and YF-XL-ΔRYF fell within the expected variability for isolates with standard 3′ NCR conformations.

The biological function of the domain I RYFs has been the source of much speculation. Because the RYF copy numbers of the major lineages of YFV (49) that are vectored by different mosquito genera differ, vector coadaptation has been pos-

tulated. Recent mutagenesis experiments using the 17D infectious clone demonstrated that all three copies of the RYF motif could be deleted without eliminating virus replication in vertebrate cell culture (3). The present study extends those observations considerably, providing mouse neuroinvasiveness and mosquito infectivity data indicating that RYF motifs are not required for in vivo replication in either vertebrate or arthropod hosts and that phenotypic differences from YF-std isolates, if any exist, are subtle (they were not detected in our experiments).

The failure to identify pronounced phenotypic differences among YF-XL, YF-XL-ΔRYF, and YF-std in these model systems does not negate the possibility that there are as-yet-undiscovered phenotypic differences in the pathogeneses, virulences, or transmissibilities of these isolates. It seems reasonable to hypothesize that the variant 3′ NCR conformations of YF-XL-ΔRYF and YF-XL viruses must confer a fitness advantage during in vivo replication under some circumstances, as otherwise they would not be retained within the lineage of wild-type circulating viruses. Although it is tempting to speculate that differing 3′ NCR conformations reflect adaptation to novel arthropod vectors or to altered transmission cycles, there is no evidence at this point to support such claims. Future studies using reverse-genetics techniques and alternative measures of replication efficiency and/or infectivity may provide more refined assessments of the phenotypic effects conferred by YF-XL and YF-XL-ΔRYF 3′ NCR conformations.

The identification of YF-XL strains may have important evolutionary implications for the virus, insofar as it provides evidence that intra- or intermolecular reactions akin to recombination have occurred at least once in the recent history of YFV. Recombinational insertions similar to the YF-XL duplication have been described for a large number of positive-sense RNA viruses; several studies have identified recombination hot spots in the 3′ NCR that correspond to direct imperfect sequence repeats, stem-loop structures, and cryptic promoter-like elements recognized by the RNA-dependent RNA polymerase (15, 40, 51). It is worth noting that until 1999, there was no evidence for recombination among flaviviruses. Since the first report of mosaic genomes among selected strains of dengue type 2 virus in 1999, examples of homologous recombination have been proposed for all four dengue viruses (42, 43, 46, 53), Japanese encephalitis virus, and St. Louis encephalitis virus (45), as well as for other viruses in the family *Flaviviridae*, including pestiviruses (bovine viral diarrhea virus) (2), hepaciviruses (hepatitis C virus) (16), and GB virus C/hepatitis C (52). Identification of recombinant (mosaic) forms of flaviviruses has been controversial, however, due to issues of strain identification and potential contamination. Furthermore, the evolutionary importance of recombination continues to be debated, as these events are believed to be extremely rare in nature and most frequently have a deleterious effect on virus fitness (27, 38). Key areas for future research include determining the mechanism by which 3′ NCR duplications are generated and maintained within virus populations, continued investigations of the phenotypic importance of 3′ NCR variations, and elucidation of the precise regulatory role of RNA secondary structures.

ACKNOWLEDGMENTS

We thank Robert Tesh and John Roehrig, who provided virus isolates from collections maintained at the World Arbovirus Reference Collection at the University of Texas Medical Branch, Galveston, Tex.; the Centers for Disease Control and Prevention, Fort Collins, Colo.; and the Instituto Evandro Chagas in Belém, Brazil, respectively. We thank the University of Texas Medical Branch Protein Core Facility for conducting sequencing reactions.

This research was supported by the CDC Fellowship Training Program in Vector-Borne Infectious Diseases no. T01/CCT622892 and by the Zelda Zinn Casper fund for graduate research. The participation of P. F. C. Vasconcelos had the financial support of a 2002 Lancet International Fellowship Award and CNPq (process 302770/02-0).

REFERENCES

1. **Armstrong, P. M., and R. Rico-Hesse.** 2001. Differential susceptibility of *Aedes aegypti* to infection by the American and Southeast Asian genotypes of dengue type 2 virus. Vector Borne Zoonotic Dis. **1:**159–168.
2. **Becher, P., M. Orlich, and H. J. Thiel.** 2001. RNA recombination between persisting pestivirus and a vaccine strain: generation of cytopathogenic virus and induction of lethal disease. J. Virol. **75:**6256–6264.
3. **Bredenbeek, P. J., E. A. Kooi, and B. D. Lindenbach.** 2003. A stable full-length yellow fever virus cDNA clone and the role of conserved RNA elements in flavivirus replication. J. Gen. Virol. **84:**1261–1268.
4. **Bryant, J. E., and A. D. T. Barrett.** 2003. Comparative phylogenies of yellow fever isolates from Peru and Brazil. FEMS Immunol. Med. Microbiol. **39:** 103–118.
5. **Charlier, N., P. Leyssen, C. W. Pleij, P. Lemey, F. Billoir, K. Van Laethem, A. M. Vandamme, E. De Clercq, X. de Lamballerie, and J. Neyts.** 2002. Complete genome sequence of Montana Myotis leukoencephalitis virus, phylogenetic analysis and comparative study of the 3′ untranslated region of flaviviruses with no known vector. J. Gen. Virol. **83:**1875–1885.
6. **Cologna, R., and R. Rico-Hesse.** 2003. American genotype structures decrease dengue virus output from human monocytes and dendritic cells. J. Virol. **77:**3929–3938.
7. **de Filippis, A. M., R. M. Nogueira, H. G. Schatzmayr, D. S. Tavares, A. V. Jabor, S. C. Diniz, J. C. Oliviera, E. Moreira, M. P. Miagostovich, E. V. Costa, and R. Galler.** 2002. Outbreak of jaundice and hemorrhagic fever in the Southeast of Brazil in 2001: detection and molecular characterization of yellow fever virus. J. Med. Virol. **68:**620–627.
8. **Deubel, V., and M.-T. Drouet.** 1997. Biological and molecular variations of yellow fever virus strains, p. 157–164. *In* J. F. Saluzzo and B. Dodet (ed.), Factors in the emergence of arbovirus diseases. Elsevier, Paris, France.
9. **Deubel, V., M. Huerre, G. Cathomas, M. T. Drouet, N. Wuscher, B. Le Guenno, and A. F. Widmer.** 1997. Molecular detection and characterization of yellow fever virus in blood and liver specimens of a non-vaccinated fatal human case. J. Med. Virol. **53:**212–217.
10. **Durbin, A. P., R. A. Karron, W. Sun, D. W. Vaughn, M. J. Reynolds, J. R. Perreault, B. Thumar, R. Men, C. J. Lai, W. R. Elkins, R. M. Chanock, B. R. Murphy, and S. S. Whitehead.** 2001. Attenuation and immunogenicity in humans of a live dengue virus type-4 vaccine candidate with a 30 nucleotide deletion in its 3′-untranslated region. Am. J. Trop. Med. Hyg. **65:**405–413.
11. **Fitzgeorge, R., and C. J. Bradish.** 1980. The *in vitro* differentiation of strains of yellow fever virus in mice. J. Gen. Virol. **46:**1–13.
12. **Gritsun, T. S., K. Venugopal, P. M. Zanotto, M. V. Mikhailov, A. A. Sall, E. C. Holmes, I. Polkinghorne, T. V. Frolova, V. V. Pogodina, V. A. Lashkevich, and E. A. Gould.** 1997. Complete sequence of two tick-borne flaviviruses isolated from Siberia and the UK: analysis and significance of the 5′ and 3′-UTRs. Virus Res. **49:**27–39.
13. **Heraud, J. M., D. Hommel, A. Hulin, V. Deubel, J. D. Poveda, J. L. Sarthou, and A. Talarmin.** 1999. First case of yellow fever in French Guiana since 1902. Emerg. Infect. Dis. **5:**429–432.
14. **Higgs, S. T., J. O. Rayner, K. E. Olson, B. S. Davis, B. J. Beaty, and C. Blair.** 1998. Engineered resistance in *Aedes aegypti* to a West African and a South American strain of yellow fever virus. Am. J. Trop. Med. Hyg. **58:**663–670.
15. **Hill, K. R., M. Hajjou, J. Y. Hu, and R. Raju.** 1997. RNA-RNA recombination in Sindbis virus: roles of the 3′ conserved motif, poly(A) tail, and nonviral sequences of template RNAs in polymerase recognition and template switching. J. Virol. **71:**2693–2704.
16. **Kalinina, O., H. Norder, S. Mukomolov, and L. O. Magnius.** 2002. A natural intergenotypic recombinant of hepatitis C virus identified in St. Petersburg. J. Virol. **76:**4034–4043.
17. **Leitmeyer, K. C., D. W. Vaughn, D. M. Watts, R. Salas, I. Villalobos de Chacon, C. Ramos, and R. Rico-Hesse.** 1999. Dengue virus structural differences that correlate with pathogenesis. J. Virol. **73:**4738–4747.
18. **Lin, K.-C., H. Chang, and R.-Y. Chang.** 2004. Accumulation of a 3′-terminal genome fragment in Japanese encephalitis virus-infected mammalian and mosquito cells. J. Virol. **78:**5133–5138.
19. **Lo, M. K., M. Tilgner, K. A. Bernard, and P. Y. Shi.** 2003. Functional analysis of mosquito-borne flavivirus conserved sequence elements within 3′ untrans-

lated region of West Nile virus by use of a reporting replicon that differentiates between viral translation and RNA replication. J. Virol. **77:**10004–10014.

20. **Markoff, L.** 2004. 5′ and 3′-noncoding regions in flavivirus RNA, p. 177–229. *In* T. J. Chambers and T. P. Monath (ed.), The flaviviruses: structure, replication, and evolution. Elsevier Press, Amsterdam, The Netherlands.
21. **Markoff, L., X. Pang, H. S. Houng, B. Falgout, R. Olsen, E. Jones, and S. Polo.** 2002. Derivation and characterization of a dengue type 1 host range-restricted mutant virus that is attenuated and highly immunogenic in monkeys. J. Virol. **76:**3318–3328.
22. **Men, R., M. Bray, D. Clark, R. M. Chanock, and C. Lai.** 1996. Dengue type 4 virus mutants containing deletions in the 3′ noncoding region of the RNA genome: analysis of growth restriction in cell culture and altered viremia pattern and immunogenicity in rhesus monkeys. J. Virol. **70:**3930–3937.
23. **Miller, B. R., and D. Adkins.** 1988. Biological characterization of plaque-size variants of yellow fever virus in mosquitoes and mice. Acta Virol. **32:**227–234.
24. **Miller, B. R., and M. E. Ballinger.** 1988. *Aedes albopictus* mosquitoes introduced into Brazil: vector competence for yellow fever and dengue viruses. Trans. R. Soc. Trop. Med. Hyg. **82:**476–477.
25. **Miller, B. R., and C. J. Mitchell.** 1986. Passage of yellow fever virus: its effect on infection and transmission rates in *Aedes aegypti*. Am. J. Trop. Med. Hyg. **35:**1302–1309.
26. **Mitchell, C. J., B. R. Miller, and D. J. Gubler.** 1987. Vector competence of *Aedes albopictus* from Houston, Texas, for dengue serotypes 1 to 4, yellow fever and Ross River viruses. J. Am. Mosquito Control Assoc. **3:**460–465.
27. **Murhpy, B. R., J. E. Blaney, Jr., and S. S. Whitehead.** 2004. Arguments for live flavivirus vaccines. Lancet **364:**499–500.
28. **Mutebi, J. P., R. C. A. Rijnbrand, H. Wang, K. Ryman, E. Wang, L. D. Fulop, R. Titball, and A. D. T. Barrett.** 2004. Genetic relationships and evolution of genotypes of yellow fever virus and other members of the yellow fever virus group within the *Flavivirus* genus based on the 3′ noncoding region. J. Virol. **78:**9652–9665.
29. **Mutebi, J. P., H. Wang, L. Li, J. E. Bryant, and A. D. Barrett.** 2001. Phylogenetic and evolutionary relationships among yellow fever virus isolates in Africa. J. Virol. **75:**6999–7008.
30. **Olsthoorn, R. C., and J. F. Bol.** 2001. Sequence comparison and secondary structure analysis of the 3′ noncoding region of flavivirus genomes reveals multiple pseudoknots. RNA **7:**1370–1377.
31. **Peerenboom, E., V. Jacobi, E. J. Cartwright, M. Adams, H.-H. Steinbiss, and J. F. Antoiw.** 1997. A large duplication in the 3′-untranslated region of a subpopulation of RNA2 of the UK-M isolate of barley mild mosaic bymovirus. Virus Res. **47:**1–6.
32. **Poidinger, M., R. A. Hall, and J. S. Mackenzie.** 1996. Molecular characterization of the Japanese encephalitis serocomplex of the Flavivirus genus. Virology **218:**417–421.
33. **Proutski, V., M. W. Gaunt, E. A. Gould, and E. C. Holmes.** 1997. Secondary structure of the 3′-untranslated region of yellow fever virus: implications for virulence, attenuation and vaccine development. J. Gen. Virol. **78:**1543–1549.
34. **Proutski, V., E. A. Gould, and E. C. Holmes.** 1997. Secondary structure of the 3′ untranslated region of flaviviruses: similarities and differences. Nucleic Acids Res. **25:**1194–1202.
35. **Proutski, V., T. S. Gritsun, E. A. Gould, and E. C. Holmes.** 1999. Biological consequences of deletions within the 3′-untranslated region of flaviviruses may be due to rearrangements of RNA secondary structure. Virus Res. **64:**107–123.
36. **Rauscher, S., C. Flamm, C. W. Mandl, F. X. Heinz, and P. F. Stadler.** 1997. Secondary structure of the 3′-noncoding region of flavivirus genomes: comparative analysis of base pairing probabilities. RNA **3:**779–791.
37. **Reed, L. J., and H. Muench.** 1938. A simple method of estimating fifty per cent endpoints. Am. J. Hyg. **27:**493–497.

37a. **Rice, C. M., E. M. Lenches, S. R. Eddy, S. J. Shin, R. L. Sheets, and J. H. Strauss.** 1985. Nucleotide sequence of yellow fever virus: implications for flavivirus gene expression and evolution. Science **229:**726–733.

38. **Seligman, S. J., and E. A. Gould.** 2004. Live flavivirus vaccines: reasons for caution. Lancet **363:**2073–2075.
39. **Shurtleff, A. C., D. W. Beasley, J. J. Chen, H. Ni, M. T. Suderman, H. Wang, R. Xu, E. Wang, S. C. Weaver, D. M. Watts, K. L. Russell, and A. D. Barrett.** 2001. Genetic variation in the 3′ non-coding region of dengue viruses. Virology **281:**75–87.
40. **Song, C., and A. E. Simon.** 1995. Requirement of a 3′-terminal stem-loop in in vitro transcription by an RNA-dependent RNA polymerase. J. Mol. Biol. **254:**6–14.
41. **Swofford, D. L.** 1998. PAUP*. Phylogenetic analysis using parsimony (* and other methods). Sinauer Associates, Sunderland, Mass.
42. **Tolou, H., P. Couissinier-Paris, V. Mercier, M. R. Pisano, X. de Lamballerie, P. de Micco, and J. P. Durand.** 2000. Complete genomic sequence of a dengue type 2 virus from the French West Indies. Biochem. Biophys. Res. Commun. **277:**89–92.
43. **Tolou, H., J. Nicoli, and C. Chastel.** 2002. Viral evolution and emerging viral infections: what future for the viruses? A theoretical evaluation based on informational spaces and quasispecies. Virus Genes **24:**267–274.
44. **Troyer, J. M., K. A. Hanley, S. S. Whitehead, D. Strickman, R. A. Karron, A. P. Durbin, and B. R. Murphy.** 2001. A live attenuated recombinant dengue-4 virus vaccine candidate with restricted capacity for dissemination in mosquitoes and lack of transmission from vaccinees to mosquitoes. Am. J. Trop. Med. Hyg. **65:**414–419.
45. **Twiddy, S. S., and E. C. Holmes.** 2003. The extent of homologous recombination in members of the genus Flavivirus. J. Gen. Virol. **84:**429–440.
46. **Uzcategui, N. Y. C.** 2001. Molecular epidemiology of dengue type 2 virus in Venezuela: evidence for in situ virus evolution and recombination. J. Gen. Virol. **82:**2945–2953.

46a. **Vasconcelos, P. F. C., J. E. Bryant, A. P. A. T. Rosa, R. B. Tesh, S. G. Rodrigues, and A. D. T. Barrett.** 2004. Genetic divergence and dispersal of yellow fever virus in Brazil: periodic expansions of the enzootic zone. Emerg. Infect. Dis. **10:**1578–1584.

47. **Wallner, G., C. W. Mandl, M. Ecker, H. Holzmann, K. Stiasny, C. Kunz, and F. X. Heinz.** 1996. Characterization and complete genome sequences of high- and low-virulence variants of tick-borne encephalitis virus. J. Gen. Virol. **77:**1035–1042.
48. **Wallner, G., C. W. Mandl, C. Kunz, and F. X. Hienz.** 1995. The flavivirus 3′-non coding region: extensive size heterogeneity independent of evolutionary relationships among strains of tick-borne encephalitis virus. Virology **213:**169–178.
49. **Wang, E., S. C. Weaver, R. E. Shope, R. B. Tesh, D. M. Watts, and A. D. Barrett.** 1996. Genetic variation in yellow fever virus: duplication in the 3′ noncoding region of strains from Africa. Virology **225:**274–281.

49a. **Wang, E., K. D. Ryman, A. D. Jennings, D. J. Wood, F. Taffs, P. D. Minor, P. G. Sanders, and A. D. Barrett.** 1995. Comparison of the genomes of the wild-type French viscerotropic strain of yellow fever virus with its vaccine derivative French neurotropic vaccine. J. Gen. Virol. **76:**2749–2755.

50. **Watts, D., G. Ramirez, C. Cabezas, M. Wooster, C. Carrillo, C. Chuy, E. J. Gentrau, and C. G. Hayes.** 1998. Arthropod-borne viral diseases in Peru, p. 193–218. *In* A. P. A. Travassos da Rosa, P. F. C. Vasconcelos, and J. F. S. Travassos da Rosa (ed.), An overview of arbovirology in Brazil and neighboring countries. Instituto Evandro Chagas, Belem, Brazil.
51. **White, K. A., and T. J. Morris.** 1995. RNA determinants of junction site selection in RNA virus recombinants and defective interfering RNAs. RNA **1:**1029–1040.
52. **Worobey, M., and E. C. Holmes.** 2001. Homologous recombination in GB virus C/hepatitis G virus. Mol. Biol. Evol. **18:**254–261.
53. **Worobey, M., A. Rambaut, and E. C. Holmes.** 1999. Widespread intraserotype recombination in natural populations of dengue virus. Proc. Natl. Acad. Sci. USA **96:**7352–7357.